Bayer Pattern CFA Demosaicking Based on Multi-Directional Weighted Interpolation and Guided Filter

Lei Wang, *Member, IEEE*, and Gwanggil Jeon, *Member, IEEE*

***Abstract*—In this letter, we proposed a new framework for color image demosaicking by using different strategies on green (G) and red/blue (R/B) components. Firstly, for G component, the missing samples are estimated by eight-direction weighted interpolation via exploiting spatial and spectral correlations of neighboring pixels. The G plane can be well reconstructed by considering the joint contribution of pre-estimations along eight interpolation directions with different weighting factors. Secondly, we estimate R/B components using guided filter with the reconstructed G plane as guidance image. Simulation results verify that, the proposed framework performs better than state-of-the-art demosaicking methods in term of color peak signal-to-noise ratio (CPSNR) and feature similarity index measure (FSIM), as well as higher visual quality.**

***Index Terms*—Bayer pattern, demosaicking, directional interpolation, guided filter.**

I. Introduction

CONSIDERING the high cost and large space of using three sensors, a single sensor is always used in digital color cameras to capture images with a color filter array (CFA). This technology is widely applied in digital imaging industry, such as smart phones. One of the most popular color arrangement patterns for the CFA in digital cameras is Bayer pattern [1], which is shown in Fig. 1. In this pattern, one quarter of the pixels measure each of R/B components, and half the pixels measure G components, since that the human eye can discern a wider range of green than red and blue colors. Only one of the three-color elements (R/G/B) is sampled at each pixel location, so the missing two color elements have to be estimated to reconstruct full color images. This process is usually called demosaicking [2].

Manuscript received May 06, 2015; revised July 09, 2015; accepted July 15, 2015. Date of publication July 21, 2015; date of current version July 24, 2015. This work was supported in part by National Natural Science Foundation of China under Grant 61302063, and by the National Research Foundation of Korea (NRF), funded by the Korean Government (MSIP), under Grant 2014025627. The associate editor coordinating the review of this manuscript and approving it for publication was Prof. Giuseppe Scarpa.

L. Wang is with the Department of Information Science and Engineering, University of Jinan, Jinan 250022, Shandong, China (e-mail: ise_wanglei@ujn.edu.cn).

G. Jeon is with the Department of Embedded Systems Engineering, Incheon National University, Incheon, Korea (e-mail: gjeon@inu.ac.kr).

Color versions of one or more of the figures in this paper are available online at http://ieeexplore.ieee.org.

Digital Object Identifier 10.1109/LSP.2015.2458934

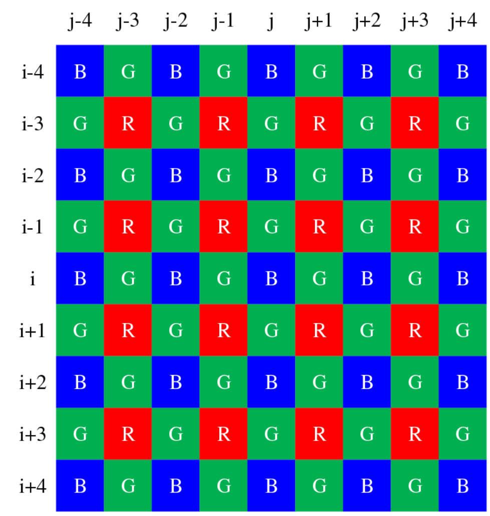

Fig. 1. Bayer CFA pattern.

In the past decades, many demosaicking methods have been developed in the aim of improving reconstruction quality of the full color image [3], [4], [5], [6], [7]. Directional interpolation methods are widely adopted since of its low complexity and satisfied performance [8], [9], [10], [11], [12], [13]. In [10], the local directional interpolation and nonlocal adaptive thresholding (LDI-NAT) method was proposed. Local directional estimations of a missing color component are computed first. To enhance the local estimate, a searching process of nonlocal similar structures is conducted. This method achieved better performance, but at the cost of higher complexity. Multi-directional weighted interpolation (MDWI) was proposed recently [13], which achieved superior performance, but a post-processing of refinement was required.

A. Our Approach

We propose a new framework for the Bayer pattern CFA demosaicking. In the first step, we view the missing G components as the expectation of a random variable $\tilde{G}^X$, which takes eight possible values with different possibilities p^X. Actually, $\tilde{G}^X$ represents pre-estimations along eight interpolation directions (i.e. N, S, W, E, NW, SW, NE, SE). Taking the missing G component at $B_{i,j}$ position for example, the estimation is formulated as follows.

$$\tilde{G}_{B_{i,j}} = \sum\nolimits_X \tilde{G}^X_{B_{i,j}} \cdot p^X. \tag{1}$$

In the second step, we estimate R/B plane using guided filter with the reconstructed G plane as guidance. Taking R plane for illustration, the primary filtering is defined as

$$\hat{R} = a \cdot \tilde{G} + b, \tag{2}$$

where (a, b) are linear coefficients in a local window. This local linear model ensures that $\hat{R}$ has an edge if only $\tilde{G}$ has an edge in the local window, since $\nabla\hat{R} = \nabla\tilde{G}$. $\hat{R}$ is viewed as a pre-estimation of R plane, which can be further improved by residual interpolation [14]. We calculate the residual between the original and pre-estimation at R position, and interpolate the missing residual components at B and G positions. Finally, we reconstruct R plane by adding the residual to the pre-estimation.

B. Relations with Existing Works

The Multi-directional weighted interpolation (MDWI) method [13] is efficient for G component, but not very good for R/B components. MDWI has not well exploited the horizontal or vertical correlations when interpolating the R/B components. In contrast, our proposed framework takes full considerations of image structures by upsampling R/B samples with reconstructed G plane as guidance. It is also related to the minimized-Laplacian residual interpolation (MLRI) [15], which estimated color planes with each other as guidance. However, our strategy of computing expectation of the missing G component with eight possibilities is more straightforward and efficient.

C. Organization

The rest of the letter is organized as follows. Section II describes the proposed demosaicking framework. Section III presents experimental results. Section IV offers a brief conclusion.

II. Proposed Framework

In this section, we introduce the realization of the proposed method. Firstly, we estimate G component by computing its expectation with eight possible values, which are pre-estimations along eight directions. Secondly, we estimate R/B components using the guided filter.

A. Estimation of Green Component

Without loss of generality, we take the estimation of the missing green component $\tilde{G}_{B_{i,j}}$ at $B_{i,j}$ position to illustrate how the method works. In fact, the joint contribution of eight pre-estimations around $B_{i,j}$ along eight directions with different factors are used for reconstructing the missing green component. The estimation is formulated as

$$\tilde{G}_{B_{i,j}} = \sum\nolimits_X \tilde{G}^X_{B_{i,j}} \cdot p_X = \frac{\sum_X \tilde{G}^X_{B_{i,j}} \cdot \omega^X}{\sum_X \omega^X}, \tag{3}$$

where X $\in$ $\{N, S, W, E, NW, SW, NE, SE\}$, $\tilde{G}^X_{B_{i,j}}$ represents the pre-estimation along X direction, and ω^X is the responding weighting factor. $\tilde{G}^X_{B_{i,j}}$ is computed by exploiting the spectral and spatial correlations, and ω^X is computed based on the edge gradient.

The pre-estimations $\tilde{G}^X_{B_{i,j}}$ along horizontal and vertical directions (i.e. N, S, W, E) are computed by exploiting spectral correlations as follows.

$$\begin{aligned} \tilde{G}^W_{B_{i,j}} &= G_{i,j-1} + (B_{i,j} - B_{i,j-2})/2, \\ \tilde{G}^E_{B_{i,j}} &= G_{i,j+1} + (B_{i,j} - B_{i,j+2})/2, \\ \tilde{G}^N_{B_{i,j}} &= G_{i-1,j} + (B_{i,j} - B_{i-2,j})/2, \\ \tilde{G}^S_{B_{i,j}} &= G_{i+1,j} + (B_{i,j} - B_{i+2,j})/2. \end{aligned} \tag{4}$$

The pre-estimations $\tilde{G}^X_{B_{i,j}}$ along four diagonal directions are computed as

$$\tilde{G}^X_{B_{i,j}} = \sum_{k=1}^{8} S^X_G(k) \cdot h_8(k), X \in \{NW, SW, NE, SE\}, \tag{5}$$

where $S^X_G(k)$ represents neighboring pixel-sets along diagonal directions, and $h_8(k)$ represents an 8-tap interpolation filter. The filter is defined as Eq. (6), which is also adopted by the latest video coding standard (HEVC) to upsample sub-pixels for more accurate prediction.

$$h_8(k) = [-1, 4, -11, 40, 40, -11, 4, -1]/64. \tag{6}$$

In Bayer pattern, the green component is continuously distributed along the diagonal direction, as shown in Fig. 2. As a result, the pixel-sets S^X_G along NW, NE, SW and SE contain useful information for the center missing green component $\tilde{G}_{B_{i,j}}$. So we use these pixel-sets for estimation, and the pixel-set along NW direction is given as follows, while the other three can be obtained in the same way as shown in Fig. 2.

$$\begin{aligned} S^{NW}_G = \{&G_{i-4,j+3}, G_{i-3,j+2}, G_{i-2,j+1}, G_{i-1,j}, \\ &\times G_{i,j-1}, G_{i+1,j-2}, G_{i+2,j-3}, G_{i+3,j-4}\}. \end{aligned} \tag{7}$$

Now we have obtained eight pre-estimations of $\tilde{G}_{B_{i,j}}$ along eight directions, and they are $\tilde{G}^N_{B_{i,j}}$, $\tilde{G}^S_{B_{i,j}}$, $\tilde{G}^W_{B_{i,j}}$, $\tilde{G}^E_{B_{i,j}}$, $\tilde{G}^{NW}_{B_{i,j}}$, $\tilde{G}^{NE}_{B_{i,j}}$, $\tilde{G}^{SW}_{B_{i,j}}$, $\tilde{G}^{SE}_{B_{i,j}}$, respectively. To guarantee an accurate final estimation, we need to determine the pre-estimations, possibility in the joint contribution. In other words, different weighting factors are required, which are defined as

$$\omega^X = \frac{1}{\nabla^X}, X \in \{N, S, W, E, NW, SW, NE, SE\}, \tag{8}$$

where ∇ represents directional gradient factors which are calculated as follows. Taking north (N) and northwest (NW) directions for illustration, gradient factors along other directions can be obtained in the symmetrical or perpendicular areas.

$$\begin{aligned} \nabla^N_{B_{i,j}} = &|G_{i-2,j-1} - G_{i,j-1}| + |G_{i-3,j} - G_{i-1,j}| \\ &+ |G_{i-2,j+1} - G_{i,j+1}| + |R_{i-3,j-1} - R_{i-1,j-1}| \\ &+ |R_{i-3,j1} - R_{i-1,j+1}| + |B_{i-2,j} - B_{i,j}| + \varepsilon, \end{aligned} \tag{9}$$

$$\begin{aligned} \nabla^{NW}_{B_{i,j}} = &|G_{i-2,j-1} - G_{i-1,j}| + |G_{i-1,j} - G_{i,j+1}| \\ &+ |G_{i-1,j-2} - G_{i,j-1}| + |G_{i,j-1} - G_{i+1,j}| \\ &+ |R_{i-1,j-1} - R_{i+1,j+1}| + |B_{i-2,j-2} - B_{i,j}| + \varepsilon, \end{aligned} \tag{10}$$

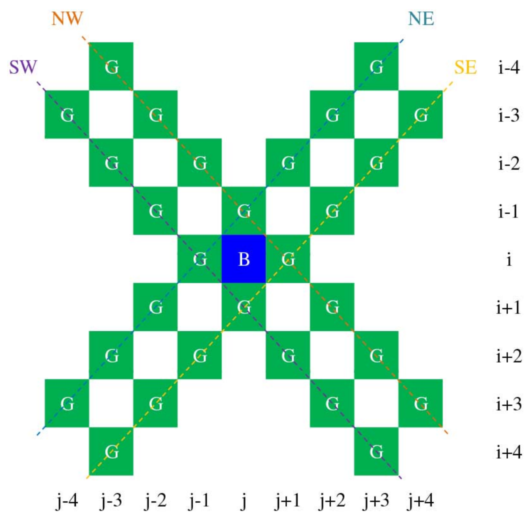

Fig. 2. Diagonal direction information.

where ε is a small positive factor to avoid the gradients being zero.

With the pre-estimations $\tilde{G}^X_{B_{i,j}}$ and the weighting factors ω^X, we can compute the final estimation $\tilde{G}_{B_{i,j}}$ using Eq. (3) for the missing G components at B position. The missing G component at R position can be estimated in the same way.

B. Estimation of Red and Blue Components

After reconstructing the G plane, we estimate R/B components using guided filter instead of directional interpolation. The guided filter is a type of simple and effective filter with edge-preserving smoothing property [16]. We take the R plane to illustrate how to realize estimation.

With the reconstructed G plane as a guidance image, a pre-estimation of the R image is generated by using the guided filter firstly. Then, we calculate the residuals between the original and the pre-estimated R pixel values at R positions. And the missing components of residuals at G/B positions are interpolated. Finally, we add the pre-estimation of the R image to the interpolated residual image to acquire the final estimated R image.

Firstly, we introduce how to get the pre-estimation of the R image by the guided filter. The reconstructed G plane is used as the guidance image, and original R samples as filter input. Then the guided filter outputs pre-estimated $\hat{R}$, which can be obtained as

$$\hat{R}_{i,j} = a_{m,n} \cdot \tilde{G}_{i,j} + b_{m,n}, \forall i,j \in W_{m,n}, \tag{11}$$

where $(a_{m,n}, b_{m,n})$ are some linear coefficients assumed to be constant in a local window $W_{m,n}$, and they are determined by minimizing the difference between output $\hat{R}$ and input R, which is expressed in the form of following cost function.

$$E(a_{m,n}, b_{m,n}) = \sum_{i,j \in W_{m,n}} \left\{ \left(a_{m,n} \cdot \tilde{G}_{i,j} + b_{m,n} - R_{i,j} \right)^2 + \xi \cdot a^2_{m,n} \right\}, \tag{12}$$

where ξ is a regularization parameter which affects the preserving of edges. $a_{m,n}$ and $b_{m,n}$ can be figured out by linear regression as

$$a_{m,n} = \frac{\frac{1}{N_W}\left(\sum_{i,j \in W_{m,n}} \tilde{G}_{i,j} \cdot R_{i,j} \right) - \mu_{m,n} \cdot \bar{R}_{m,n}}{\sigma^2_{m,n} + \xi}, \tag{13}$$

$$b_{m,n} = \bar{R}_{m,n} - a_{m,n} \cdot \mu_{m,n}, \tag{14}$$

where $\mu_{m,n}$ and $\sigma^2_{m,n}$ are the mean and variance of $\tilde{G}$ in $W_{m,n}$, N_W is the number of pixels in $W_{m,n}$, and $\bar{R}_{m,n} = (\sum_{i,j \in W_{m,n}} R_{i,j})/N_W$ is the mean of R in $W_{m,n}$. In our experiment, the size of the local window is set to be 5, and the regularization parameter ξ is set to be 0.01.

Secondly, we further improve the pre-estimation by the following process. We calculate the residuals between the original and the pre-estimated R pixel values at R positions.

$$D_{R(i,j)} = R_{i,j} - \hat{R}_{i,j}. \tag{15}$$

And the missing components of residuals at G/B positions are interpolated.

$$D_{B(i,j)} = (D_{R(i-1,j-1)} + D_{R(i-1,j+1)} + D_{R(i+1,j-1)} + D_{R(i+1,j+1)})/4, \tag{16}$$

$$D_{G_H(i,j)} = (D_{R(i,j-1)} + D_{R(i,j+1)})/2, \tag{17}$$

$$D_{G_V(i,j)} = (D_{R(i-1,j)} + D_{R(i+1,j)})/2, \tag{18}$$

where $D_{G_H(i,j)}$ and $D_{G_V(i,j)}$ are the missing components of residuals at G positions along horizontal and vertical directions, respectively. Finally, we add the pre-estimation of the R image to the interpolated residual image to acquire the final estimated R plane.

$$\tilde{R}_{i,j} = \hat{R}_{i,j} + D_{i,j}. \tag{19}$$

The blue plane can be estimated in the same way using guided filter with the reconstructed G plane as a guidance image.

III. Experiments and Discussions

To validate the proposed framework, we did experiments and compared its performance against state-of-the-art methods; DLMMSE [9], LDI-NAT [10], MDWI [13] and MLRI [15]. MDWI with no refinement (MDWI$_N$) [13] was also compared.

The McMaster (McM) and Kodak dataset were used in our experiments, which have been widely adopted for assessing the efficiency of demosaicking methods. Our experiments were performed in MATLAB R2013 with a processor of Intel(R) Core(TM) i5-3570 CPU@3.40GHZ.

Firstly, the comparison is made in term of the color peak signal-to-noise ratio (CPSNR). The results have been listed in Table I. From Table I, we can see that, no one method performs best on all images. The proposed method obtained the best results on 4 images. And its performance is better than all the other methods except MLRI [15]. Compared with MDWI$_N$ [13], the proposed method achieved an improvement of 0.47 dB in average. In [13], the authors also proposed a refinement method after interpolation, but our method is still better than it without any post-processing.

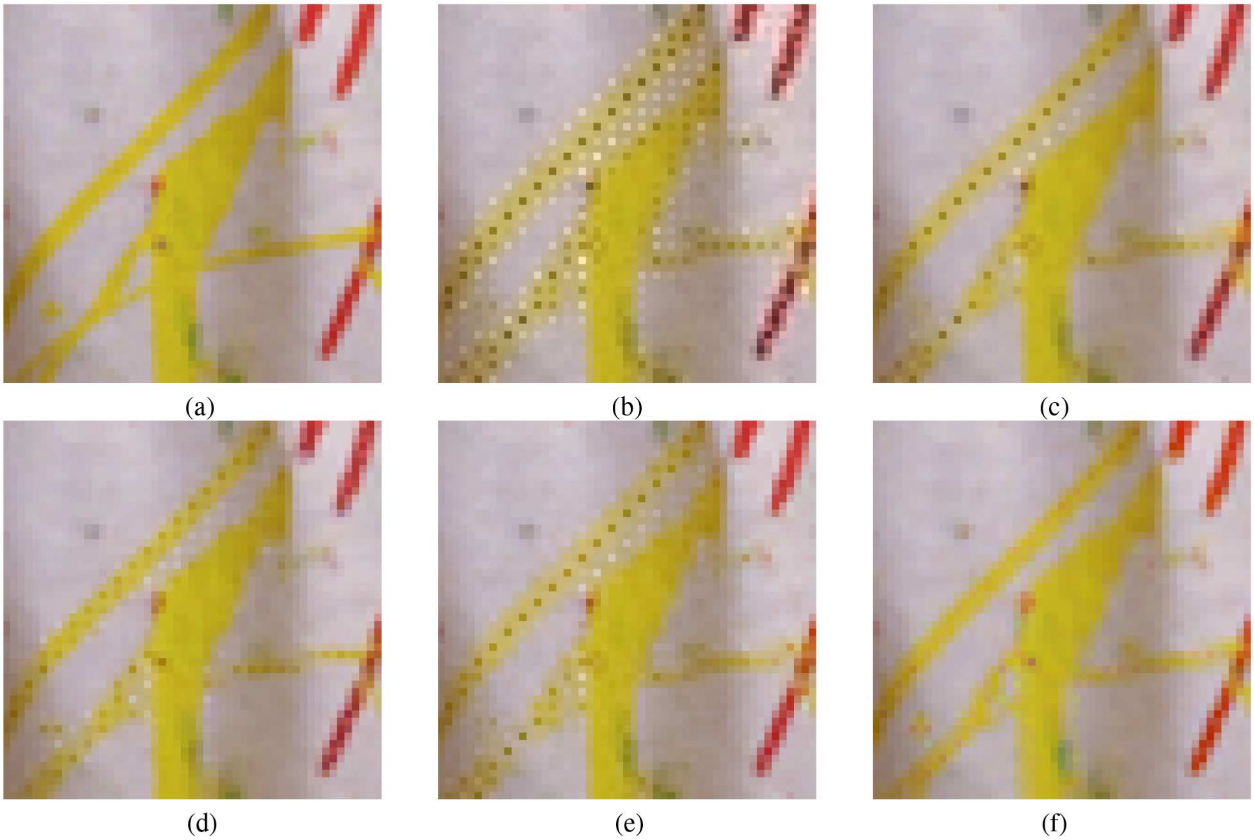

Fig. 3. Subjective quality comparison of partial No.5 image: (a) Original, (b) DLMMSE, (c) LDI-NAT, (d) MDWI, (e) MLRI, and (f) proposed.

TABLE I
CPSNR RESULTS (IN dB)

Image	DL	LDI-NAT	MDWI_N	MDWI	MLRI	Proposed
1	26.98	29.08	29.15	**29.29**	28.97	29.21
2	31.28	33.85	34.18	**34.33**	34.01	34.21
3	33.83	37.95	37.81	38.06	38.26	**38.69**
4	34.41	**37.20**	36.76	37.12	36.45	36.45
5	36.34	38.67	38.35	38.59	38.63	**38.71**
6	38.80	40.70	40.82	**40.94**	40.51	40.57
7	37.24	38.65	38.54	38.66	38.76	**38.93**
8	37.27	38.96	39.12	**39.23**	38.91	38.97
9	30.45	33.97	34.36	34.32	35.08	**35.15**
10	29.31	32.78	33.26	**33.41**	32.58	33.03
11	40.92	39.71	37.22	37.94	**40.74**	39.15
12	41.10	39.81	38.12	38.79	**41.44**	39.58
13	39.88	38.43	36.98	37.62	**39.31**	37.75
14	43.31	42.08	40.94	41.60	**43.73**	41.79
Avg.	35.79	37.28	36.83	37.14	37.67	37.30

TABLE II
FSIMC RESULTS

Image	DL	LDI-NAT	MDWI_N	MDWI	MLRI	Proposed
1	0.9923	0.9947	0.9940	0.9943	0.9944	0.9944
2	0.9968	0.9982	0.9984	0.9984	0.9983	0.9984
3	0.9981	0.9991	0.9990	0.9991	0.9990	0.9990
4	0.9969	0.9984	0.9981	0.9983	0.9978	0.9977
5	0.9982	0.9990	0.9989	0.9990	0.9989	0.9989
6	0.9981	0.9989	0.9989	0.9989	0.9989	0.9989
7	0.9980	0.9987	0.9987	0.9988	0.9986	0.9988
8	0.9979	0.9984	0.9984	0.9985	0.9983	0.9982
9	0.9973	0.9984	0.9983	0.9984	0.9982	0.9984
10	0.9945	0.9974	0.9974	0.9976	0.9968	0.9970
11	0.9984	0.9981	0.9960	0.9967	0.9984	0.9983
12	0.9991	0.9988	0.9980	0.9986	0.9992	0.9990
13	0.9985	0.9979	0.9971	0.9973	0.9983	0.9980
14	0.9993	0.9993	0.9990	0.9991	0.9994	0.9993
Avg.	0.9974	0.9982	0.9979	0.9981	0.9982	0.9982

Secondly, we tested these methods based on another criterion, feature similarity index measure for color image (FSIMc) [17]. FSIMc is an image quality assessment metric, which can achieve very high consistency with human subjective evaluations. The results have been compared in Table II. From Table II, we can see that the proposed method achieved the best performance.

Finally, we compared the subjective quality of demosaicked partial No. 2 image, as shown in Fig. 3. From Fig. 3 we can see that, the reconstructed image by our proposed method has less visual artifacts than other methods.

The computational complexity of the proposed algorithm is $O(N)$ time. It is suitable for real-time applications. In our experiments, 0.36 seconds were needed to process one image in average.

IV. CONCLUSIONS

In this letter, we have proposed a new color image demosaicking framework based on multi-directional weighted interpolation and guided filter (MDWI-GF). In the first step, we reconstruct G plane by computing the joint contribution of estimation along eight interpolation directions. In the second step, the reconstructed G plane is viewed as a guidance image for R/B plane, and the R/B plane is estimated using guided filter. The edges and textures of R/B plane can be well estimated. Simulation results have verified that, the proposed method has effectively improved the original MDWI method both objectively and subjectively.

REFERENCES

[1] B. E. Bayer, “Color imaging array,” U.S. Patent 3971065, Jul. 1976.

[2] H. J. Trussell and R. E. Hartwig, “Mathematics for demosaicking,” *IEEE Trans. Image Process.*, vol. 11, no. 4, pp. 485–492, Apr. 2002.

[3] B. K. Gunturk, J. Glotzbach, Y. Altunbasak, R. W. Schafer, and R. M. Mersereau, “Demosaicking: Color filter array interpolation,” *IEEE Signal Process. Mag.*, vol. 22, no. 1, pp. 44–54, Jan. 2005.

[4] X. Li, B. Gunturk, and L. Zhang, “Image demosaicing: A systematic survey,” in *Proc. Visual Communications and Image Processing. SPIE*, 2008, vol. 6822, p. 68221J.

[5] D. Menon and G. Calvagno, “Color image demosaicking: An overview,” *Signal Process.: Image Commun.*, vol. 26, no. 8–9, pp. 518–533, Oct. 2011.

[6] P. Getreuer, “Color demosaicking with contour stencils,” in *Proc. Int. Conf. Digital Signal Processing (DSP)*, 2011, pp. 1–6.

[7] J. Duran and A. Buades, “Self-similarity and spectral correlation adaptive algorithm for color demosaicking,” *IEEE Trans. Image Process.*, vol. 23, no. 9, pp. 4031–4040, 2014.

[8] W. Lu and Y. Tan, “Color filter array demosaicking: New method and performance measures,” *IEEE Trans. Image Processing*, vol. 12, no. 10, pp. 1194–1210, Oct. 2003.

[9] L. Zhang and X. Wu, “Color demosaicking via directional linear minimum mean square-error estimation,” *IEEE Trans. Image Process.*, vol. 14, no. 12, pp. 2167–2178, Dec. 2005.

[10] L. Zhang, X. Wu, A. Buades, and X. Li, “Color demosaicking by local directional interpolation and non-local adaptive thresholding,” *J. Electron. Imag.*, vol. 20, no. 2, p. 023016, Jun. 2011.

[11] Y. Yun, J. Bae, and J. Kim, “Multidirectional edgedirected interpolation with region division for natural images,” *Opt. Eng.*, vol. 51, no. 4, p. 040503, Apr. 2012.

[12] I. Pekkucuksen and Y. Altunbasak, “Edge strength filter based color filter array interpolation,” *IEEE Trans. Image Processing*, vol. 21, no. 1, pp. 393–397, Jan. 2012.

[13] X. Chen, G. Jeon, J. Jeong, and L. He, “Multidirectional weighted interpolation and refinement method for bayer pattern cfa demosaicking,” *IEEE Trans. Circuits Syst. Video Technol.*, 2014, doi: 10.1109/TCSVT.2014.2313896.

[14] D. Kiku, Y. Monno, M. Tanaka, and M. Okutomi, “Residual interpolation for color image demosaicking,” in *Proc. IEEE Int. Conf. Image Processing*, Sep. 2013, pp. 2304–2308.

[15] D. Kiku, Y. Monno, M. Tanaka, and M. Okutomi, “Minimized-laplacian residual interpolation for color image demosaicking,” in *Proc. IST/SPIE Electronic Imaging*, Mar. 2014, vol. 9023, pp. 90230L1–8.

[16] K. He, J. Sun, and X. Tang, “Guided image filtering,” *IEEE Trans. Patt. Anal. Mach. Intell.*, vol. 35, no. 6, pp. 1397–1409, Jun. 2013.

[17] L. Zhang, L. Zhang, X. Mou, and D. Zhang, “FSIM: A feature similarity index for image quality assessment,” *IEEE Trans. Image Process.*, vol. 20, no. 8, pp. 2378–2386, Aug. 2011.